Bioorganic & Medicinal Chemistry 16 (2008) 6611–6616

Contents lists available at ScienceDirect

Bioorganic & Medicinal Chemistry

journal homepage: www.elsevier.com/locate/bmc

High throughput solubility determination with application to selection of compounds for fragment screening

Nicola Colclough, Alison Hunter, Peter W. Kenny *, Rod S. Kittlety, Lynsey Lobedan †, Kin Y. Tam *, Mark A. Timms

AstraZeneca, Mereside, Alderley Park, Macclesfield, Cheshire SK10 4TG, UK

ARTICLE INFO

Article history:
Received 22 January 2008
Revised 2 May 2008
Accepted 7 May 2008
Available online 10 May 2008

Keywords:
Solubility
Physicochemical properties
UV/vis spectroscopy
Automation
Structure–property relationship
Fragment screening
Fragment-based drug discovery
Screening library

ABSTRACT

The development and application of a high throughput aqueous solubility assay is reported. Measurements for up to 637 compounds can be made in a fully automated experiment. Results from this assay were used to quantify risk of unacceptable solubility as a function of lipophilicity for neutral fragment-like compounds. Assessment of risk of unacceptable solubility was combined with experimental solubility measurement to select compounds for inclusion in a fragment-screening library.

1. Introduction

Aqueous solubility is a key physicochemical property in drug discovery.[1,2] Solubility is usually expressed as log*S*, where *S* is the saturated compound concentration in mol L^{-1} in equilibrium with solid under defined conditions such as physiological pH at room temperature. Typical values of log*S* for discovery compounds lie in the range −7 to −3. High solubility in intestinal fluid provides the concentration gradient that drives absorption of orally administered drugs while solubility in plasma is even more critical for intravenously administered agents. In lead discovery, poor solubility in assay buffer can make it difficult to establish structure–activity relationships (SAR). Lead discovery frequently exploits high throughput screening (HTS) to identify large numbers of potentially interesting compounds that need prioritization for more detailed evaluation. This translates into a need for physicochemical property assays with greater throughput or more reliable property prediction. Solubility is a difficult property to predict accurately because the structure of the solid state is generally unknown and the development of models remains an active area of research.[3,4]

Over the last decade a number of high throughput solubility assays have been described.[5] Lipinski pioneered the use of a turbidimetic method, which provided a fast way to rank the solubility of compounds.[1] Since then, Bevan[6] and Pan[7] have extended this light scattering approach for solubility determination. In these methods, the compound, which is pre-dissolved in dimethyl sulfoxide (DMSO), is titrated to a blank aqueous buffer. The point of precipitation is detected by turbidimetric, nephelometric or spectroscopic means and the solubility of the compound determined. However, contact time between the compound and the buffer solution tends to be in the order of minutes and the DMSO composition can vary up to 5%. Under these conditions, an enhanced solubility can be generated, which may be different from the thermodynamic solubility of the most stable crystalline form of the compound. Moreover, these techniques are generally not sensitive enough for measuring solubility below log*S* of −4.7 (ca. 20 μM).[8] Alternative approaches have been developed to overcome some of these issues.[8–11] In these studies, compounds, either pre-dissolved in solvent, for example, DMSO, or in the form of solid, are brought in contact with buffer of known pH. Equilibration time between the solid and liquid phases is between 1 and 24 h. Following the phase separation by filtration or centrifugation, the solubility can be determined by UV–visible plate reader, HPLC-based UV or MS detector. It is noted that none of these approaches is fully

* Corresponding authors. Tel.: +44 (0) 1625 514396 (P.W.K.); tel.: +44 (0) 1625 230338; fax: +44 (0) 1625 510097 (K.Y.T.).
E-mail addresses: peter.kenny@astrazeneca.com (P.W. Kenny), kin.tam@astrazeneca.com (K.Y. Tam).
† Present address: Peakdale Molecular Ltd, Peakdale Science Park, Sheffield Road, Chapel-en-le-Frith, High Peak, SK23 OPG, UK.

0968-0896/$ - see front matter © 2008 Elsevier Ltd. All rights reserved.
doi:10.1016/j.bmc.2008.05.021

automated or offers sufficient capability to enable the rapid profiling of actives from HTS.

Fragment-based drug discovery (FBDD) represents a paradigm shift in the search for new medicines in an increasingly competitive marketplace.[12–14] Currently the main focus of FBDD is lead discovery, for which the starting point is screening a library of low molecular weight compounds. The main advantages of fragment-based methods over conventional screening are that they provide access to a larger and more diverse chemical space and enable this to be searched at a more controllable resolution.[14] Fragments typically bind more weakly to their targets and must be tested at high concentration, placing demands on both assay methodology and properties of the screening library compounds, in particular aqueous solubility. Assays must be more robust and capable of quantifying weak interactions without interference so affinity methods[15] are frequently used to screen fragments. In order to exploit this emerging technology, a generic-screening library[14] (GFSL05) of 20k fragments has been assembled as a tactical component of FBDD strategy. The library has been designed to be generic with respect to both the target and the technology used to detect binding. Molecular size and complexity[16] were restricted using substructural filters encoded in the expressive SMARTS[17] notation and fingerprint methods[18] were used to provide appropriate coverage of chemical space.

Building on the work of Pan et al.,[7] Chen et al.[8] and Avdeef,[9] we describe the development of a fully automated high throughput solubility assay. A UV plate reader is used for analyte quantification and an algorithm has been developed for automated processing of spectral data. A throughput of 637 compounds per experiment can be achieved using this approach with duplicate measurements for each compound and the assay can be run unattended. The high throughout solubility assay was validated against an HPLC-based solubility assay using a set of 200 compounds. The assay was used to prioritize compounds for inclusion in a fragment-screening library by reducing risk of selecting poorly soluble fragments.

2. Results and discussion

2.1. Validation of the high throughput solubility assay

In developing the high throughput solubility assay, it was essential to evaluate the precision and accuracy of the UV plate reader. The noise level of the optical system was first established. This can be defined as the average of the standard deviation of the absorbance at 250 nm in the blank wells of a 96-well UV plate containing 1% DMSO in 0.05 M sodium phosphate buffer (pH 7.4). The standard deviation data was recorded over a period of 6 months while the assay was being developed. The average of these standard deviation values was found to be 0.009 a.u. Note that the figure quoted here only represents the lower limit of the detector. The practical lower solubility limit of the assay is strongly dependent on the molar absorption coefficient of the compound and analytical wavelength used. Compounds with large molar absorption coefficients are more easily detected than those having low molar absorption coefficients. In the subsequent discussion, we will seek to establish this from a set of in-house research compounds selected from a range of projects. To establish the upper limit of the assay and the experimental error associated with this, the solubility[19] of diclofenac ($\log S = -1.52$) has been repeatedly measured in the high throughput solubility assay. A mean $\log S$ of -4.01 ± 0.04 (±2SD) has been determined from 368 measurements, which is in excellent agreement with the theoretical maximum $\log S$ (-4.00) of the assay.

Next, a set of 200 compounds including structurally diverse in-house research compounds and commercial compounds were studied in the high throughput solubility assay. Figure 1 shows the results as determined using the high throughput solubility assay, which are consistent with those determined by the HPLC-based solubility assay using solid materials. We do not anticipate an exact 1:1 agreement between results from the two assays because of different physical forms of solid material that could be generated in the two assays. It has been reported[20] that solubilities of different polymorphs are typically within threefold of each other which is consistent with our results (see Fig. 1). Moreover, the average standard deviation from four independent assays was found to be 0.1 log units (within a factor of 1.2), suggesting that assay results are reproducible. As shown in Figure 1, there are some outliers, which exhibit a positive deviation greater than a factor of three from the data generated by the solid solubility assay. These may reflect precipitation of an amorphous form of solid in the assay, which may not equilibrate to the more stable crystalline form in 24 h. However, there is one compound (see Fig. 1, symbol in circle), for which solubility is significantly lower when measured using from DMSO solution. Additional experiments have been performed on this compound to confirm compound retention at the filtration step is insignificant. Powder X-ray diffraction experiments were performed on the precipitates generated from both the high throughput solubility assay and the solid solubility assay for this compound. As shown in Figure 2, the former is highly crystalline, while the latter is amorphous material with some crystalline character. It is likely that the highly crystalline form of the compound exhibits a much lower solubility than the amorphous form, which is consistent with our data. Based on the results obtained from this test set of 200 compounds, the lowest solubility limit is approximately 2 μM ($\log S \sim -5.7$, see Figure 1).

2.2. Use of the high throughput solubility assay in fragment selection

Fragments require good aqueous solubility but they also need to bind to their targets. While polarity and the presence of ionisable

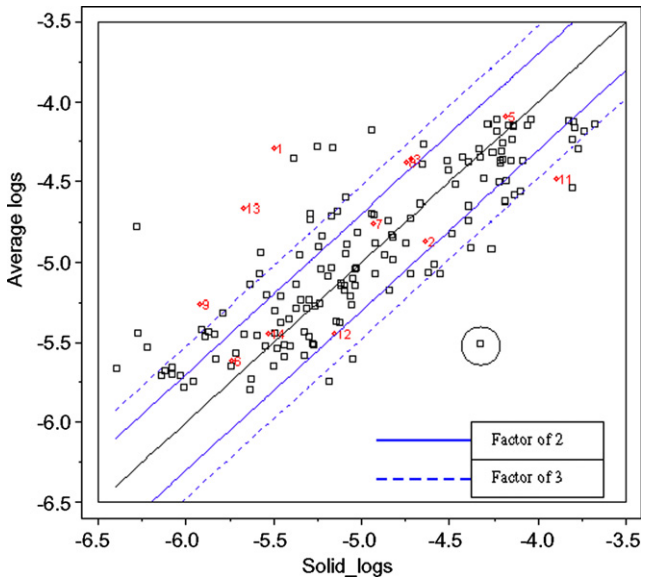

Figure 1. Correlation between the solubility of the test set obtained from the solid solubility assay (*x*-axis) and from the high throughput solubility assay (*y*-axis; average of four experiments). The black line is the 1:1 line. Symbol represents in-house compounds. Symbol ◇ represents commercial compounds: 1—disulfiram, 2—diethylstilbestrol, 3—griseofulvin, 5—haloperidol, 6—mebendazole, 7—glyburide, 8—nifedipine, 9—albendazole, 10—bumetanide analogue, 11—loperamide, 12—astemizole, 13—nimodipine, 14—loratadine. Symbol in circle represents the negative outlier as discussed in the text.

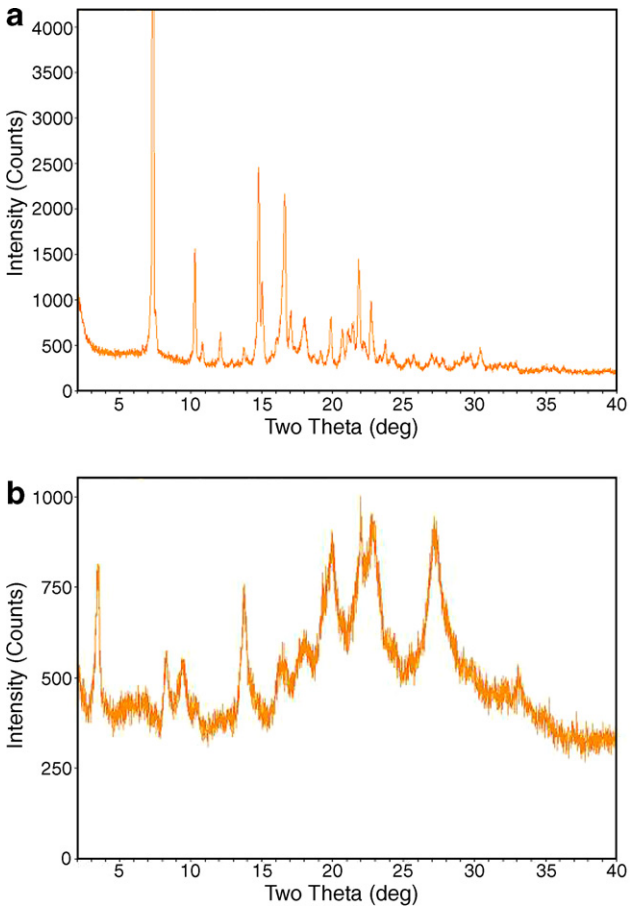

Figure 2. Powder X-ray diffraction patterns on the precipitates of the negative outlier (symbols in circle in Fig. 2, see text). (a) Generated from the high throughput solubility assay. (b) Generated from the solid solubility assay.

groups with pK_a values in the appropriate range both favor aqueous solubility, hydrophobic forces are implicated to some extent in most biomolecular recognition and a degree of hydrophobic character is necessary for binding to typical targets. The high throughput solubility assay was used both to quantify the risk of poor solubility as a function of lipophilicity and to screen compounds prior to inclusion in the library. It is noted that the assay has been designed for screening and trades off dynamic range for throughput and we require that measured solubility be at or above the upper quantification limit for a compound to be included in the fragment-screening library.

A total of 3568 solubility measurements for 3234 compounds were used as a training set to explore the relationship between solubility and lipophilicity as defined by predicted 1-octanol/water partition coefficient (C log *P*). All of these compounds were classified as neutral according to the in-house ionization and tautomer model.[21] Most (2173) of the measured solubilities exceeded the upper quantification limit of the assay while 43 measured values were below the lower limit. Measured values outside the limits of quantification cannot be used in conventional regression analysis while the alternative approach of categorizing compounds as soluble or insoluble discards information about variation in response to C log *P* across its range. The data set was partitioned by C log *P* into 10 bins, each with 356 or 357 solubility measurements and solubility was set to the appropriate assay limit when out of range. The median, 10, 20, 30 and 40 percentiles for log *S* were plotted against mean C log *P* for each bin (Fig. 3). This shows the relationship between solubility and lipophilicity in a way that discards little information and represents a general approach to analysing results from assays with limited dynamic range. We note that plotting a single percentile, such as the median, for each bin would hide intra-bin variation in log *S* and provide no information about the strength of the trend that such a plot might illustrate. Where possible, bins should be defined to include equal numbers of measurements.

Figure 3 allows the risk of poor fragment solubility to be assessed as a function of C log *P*. We used this analysis to set a threshold of 2.19 below which the risk of poor solubility would be acceptably small for neutral fragments. Once the analysis presented in Figure 3 was complete, the assay was used primarily to screen candidates for inclusion in the fragment library with C log *P* values that exceeded this threshold. It must be stressed that this approach is about managing the risk of poor fragment solubility and that we have exploited the high capacity of the assay to set a conservative threshold of 2.19. A lower assay capacity would have forced setting of a higher threshold for C log *P* and acceptance of a greater risk of poor solubility for fragments with C log *P* values below that threshold. An alternative approach could be to make the probability of selecting a fragment for assay depend on C log *P*. The solubility measurements used to derive the risk model were for low molecular weight compounds and Figure 3 has general relevance to fragment library design.

Solubility was measured for a further 2047 potential library selections and compounds were included in the library when their measured values were at or above the upper quantification limit for the assay. Most of these compounds had C log *P* values in the range 2.19–3.80, for which analysis of the training set suggested a high risk of poor solubility. These measurements can be used to validate the model and Table 1 shows good agreement between the 10% and 20% quantiles observed for log *S* in training and validation sets. The mean numbers of non-hydrogen atoms are 16.2 (SD = 4.9) in the training set and 17.0 (SD = 2.9) in the validation set and we would not expect the solubility model to be transferable to compounds of significantly different molecular size.

3. Conclusion

A high throughput solubility assay using 10 mM compound in DMSO solution has been described. An algorithm has been developed to enable automated spectral data processing and the assay is capable of measuring the solubility of 637 compounds in a single unattended experiment. Sample quantification is accomplished by

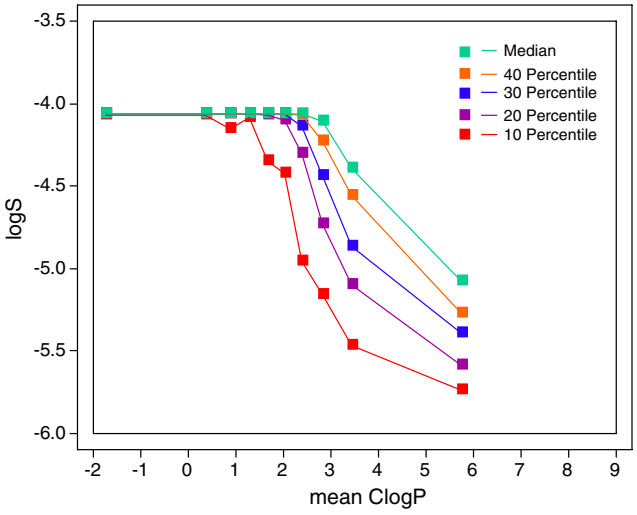

Figure 3. Percentiles for solubility for training set fragments as function of mean C log *P* for each bin.

Table 1
Comparison of 10% and 20% quantiles of log*S* for validation and training sets

Bin[a]	*N*[b]	Min C log*P*[c]	Max C log*P*[c]	log*S* 10% quantile training set	log*S* 10% quantile validation set	log*S* 20% quantile training set	log*S* 20% quantile validation set
1	45	−3.56	0.06	−4.07	−4.06	−4.06	−4.06
2	33	0.06	0.66	−4.07	−4.40	−4.06	−4.15
3	40	0.66	1.10	−4.15	−4.24	−4.06	−4.06
4	34	1.11	1.47	−4.08	−4.28	−4.06	−4.12
5	36	1.47	1.84	−4.35	−4.42	−4.07	−4.15
6	86	1.84	2.19	−4.42	−4.73	−4.10	−4.27
7	474	2.19	2.58	−4.96	−4.72	−4.30	−4.35
8	636	2.58	3.08	−5.16	−5.18	−4.73	−4.65
9	565	3.09	3.80	−5.47	−5.32	−5.10	−5.00
10	94	3.80	7.70	−5.74	−5.71	−5.59	−5.42

[a] Bin index for training set.
[b] Number of validation set compounds in bin.
[c] Bin ranges for training set.

means of a UV plate reader and the dynamic range of the assay is 2–100 μM. The assay has been validated against a traditional HPLC-based solubility assay using solid materials. Using a test set of 200 compounds, it has been shown that the agreement between these two assays is generally within threefold. A simple model has been developed to quantify risk of unacceptable solubility as a function of C log*P* for neutral fragments. Additional measurements for fragments with a high risk of poor solubility were used primarily to select library compounds but also to validate this model for fragment solubility.

4. Experimental

4.1. Chemicals used for solubility assay validation

A set of 200 compounds, including structurally diverse in-house research compounds and commercial compounds, with a wide range of solubility was used to validate the high throughput solubility assay. Sodium dihydrogen phosphate (AR grade), sodium hydroxide (AR grade), methanol (HPLC grade) and DMSO (HPLC grade) were purchased from Fisher Scientific (Loughborough, UK). Water was purified by a Millipore Milli-Q system.

4.2. Solubility assays

In the high throughput solubility assay, all compounds used were in the form of 10 mM DMSO solution in barcoded 96-well microplates. Twelve microliters of the compound solution was added to 1.2 mL of 0.05 M sodium phosphate buffer (pH 7.4) to make up 1% DMSO solutions. These solutions were then stirred using 28 mm stirring bars and a strong magnetic stirrer (model VP710E, V&P Scientific, San Diego, USA) for 24 h at 23 ± 2 °C to enable equilibration between the solid and liquid phases. Phase separation was accomplished by filtering the resultant solution through a glass fiber filter plate (Whatman unifilter, product No. 7700–7203). To minimize undesirable compound precipitation after filtration, 100 μL of the filtrate was immediately diluted by 200 μL of methanol as co-solvent. The concentration of the compound in the supernatant solution is determined by spectrophotometry with the compound at known concentration and same co-solvent composition as a reference. A Safire plate reader fitted with a DAS module (Tecan, Reading, UK) and Corning Costar UV plates (product No. 3653) were used for this purpose. The experiment was performed using a Tecan Genesis 200 Workstation equipped with a TeMo 96-headed pipette module and a Te-VacS filtration unit (Tecan, Reading, UK). All micro-plates were handled using a Kendro Cytomat 24 carousel fitted with a barcode scanner (Thermo Electron, Langenselbold, Germany). Figure 4 shows the experimental setup of the high throughout solubility assay. The experiment was fully automated using the Tecan FACTS software (flexible assay composer and task scheduler). Duplicate experiments were made for all compounds in each assay. The average of the duplicate reported if the agreement was within a factor of 2. With this set-up, the assay is able to process up to seven 96-well DMSO plates in duplicate, which allows a throughput of up to 637 solubilities per experiment in 38 h.

An algorithm has been developed for processing the spectral data generated by the high throughput solubility assay, which enabled automated processing of data without need for user intervention. The success of this approach depends strongly on the quality of the spectral data. In this study, acquisition of spectra was performed in triplicate to allow mean and standard deviation to be calculated for absorbance at each wavelength. If the standard deviation at any wavelength was found to be greater than the noise level of the optical system (see Section 2), the result for that well is rejected. The average spectral data was then background subtracted from an average of three blank wells (in the same UV plate with the same matrix compositions). Internal referencing treatment by using a 5-nm band from the visible wavelengths was then applied to the UV data. The solubility of the compound (C_{smp}) was calculated from the absorbance at the analytical wavelength using the following equation.

$$C_{\mathrm{smp}} = C_{\mathrm{std}} \left(\frac{A_{\mathrm{smp}}(\lambda_{\mathrm{anal}})/D_{\mathrm{smp}}}{A_{\mathrm{std}}(\lambda_{\mathrm{anal}})/D_{\mathrm{std}}} \right) \quad (1)$$

C_{std} is the concentration of the standard (usually 10 mM), and $A(\lambda_{\mathrm{anal}})$ is the absorbance at the analytical wavelength. D_{smp} and D_{std} are the dilution factors for sample and standard. The following rules were used to aid the selection of analytical wavelength:

1. A change of sign (from positive to negative) in the first derivative of the UV spectrum ($\mathrm{d}A/\mathrm{d}\lambda$).
2. A_{std} is greater than three times the noise level of the optical system.
3. A_{smp} is greater than the noise level of the optical system.

It is possible that a change of sign from positive to negative in the first derivative spectrum (rule (1)) is not available for a given UV spectrum because a well defined peak is not exist in the experimental wavelength region. However, rules (2) and (3) must be satisfied before a result can be accepted.

When rule (2) is not satisfied, it is normally a consequence of the extinction coefficient of the compound at the analytical wavelength being too small to be useful for quantification purpose. This spectral behavior is uncommon (typically $\leqslant$0.5% of compounds) and would be flagged as absorbance below the limited of quantification (LOQ). If A_{smp} is less than the noise level (rule (3)), the result would be quoted as under-range.

Significant mismatch between reference and sample spectra may reflect the presence of impurities, compound decomposition

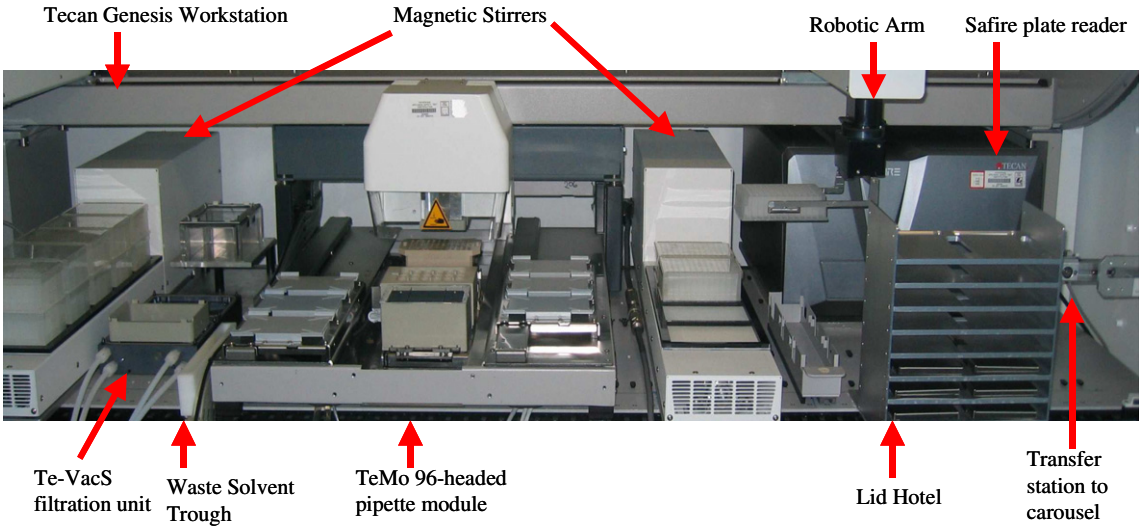

Figure 4. Experimental setup for high throughout solubility assay.

during the experiment or bubble formation in the analyte solution. The goodness-of-fit (GOF) calculation was used to quantify the correlation between the sample and the standard spectra (Eq. 2).

$$\mathrm{GOF} = \sqrt{\frac{1}{nw-1}\sum_{\lambda=\lambda 1}^{\lambda 2}\frac{\left(A_{\mathrm{smp}}(\lambda)/A_{\mathrm{smp}}(\lambda_{\mathrm{anal}}) - A_{\mathrm{std}}(\lambda)/A_{\mathrm{std}}(\lambda_{\mathrm{anal}})\right)^2}{\left((\sigma_{\mathrm{smp}}(\lambda)+\sigma_{\mathrm{smp,blk}}(\lambda))/A_{\mathrm{smp}}(\lambda_{\mathrm{anal}})\right)^2 + \left((\sigma_{\mathrm{std}}(\lambda)+\sigma_{\mathrm{std,blk}}(\lambda))/A_{\mathrm{std}}(\lambda_{\mathrm{anal}})\right)^2}} \quad (2)$$

where nw represents the number of wavelength channels used. The symbols $\sigma_{\mathrm{smp,blk}}(\lambda)$ and $\sigma_{\mathrm{std,blk}}(\lambda)$ represent the standard deviation of the blank spectra in the sample and standard plates. The wavelength channels at the start and the end of the absorption spectrum are represented by $\lambda 1$ and $\lambda 2$, respectively. Ideally each compound should have a GOF value less than or equal to one, which implies the deviation between the sample and standard spectra is less than or equal to unit variance. Analyses of data obtained from measurements of solutions with slight impurities (ca. 5%) generally show higher GOF values. A GOF greater than 5 indicates a significant mismatch between sample and standard spectra.

For comparison purposes, the set of 200 validation compounds were studied in an HPLC-based solubility assay, where the starting materials were in the form of solid. In this method, a known mass of compound (ca. 1 mg) was added to 0.1 M sodium phosphate buffer (pH 7.4) to make up a concentration of 1 mg/mL, and then stirred for 24 h at room temperature using parylene coated discs (5.3 mm) and a magnetic stirrer (model VP710E, V&P Scientific, San Diego, USA). The resulting mixture was centrifuged (Jouan Centrifuge, model Kr 4i) twice to remove any un-dissolved material. The supernatant was analyzed with an HPLC (Waters 2790) coupled with a UV diode array detector (Waters 996) and the solubility was determined by comparing the peak area of a standard solution of known concentration.

4.3. Powder X-ray diffraction

Powder X-ray diffraction (PXRD) studies were run on a Rigaku Miniflex diffractometer using Cu-Kα radiation at 1.5406 Å wavelength. The system has a variable incident slit and monochromator with a scintillation counter detector. Samples were analyzed by presenting a flat bed of powder to the beam using a silicon wafer holder. The sample was rotated at ~40 rpm to reduce crystal orientation effects. The 2θ range scanned was 2–40° with a sampling width of 0.01° and a scan speed of 0.3° min^{-1}. The PXRD patterns were recorded at ambient temperature.

4.4. Computational details

Predicted 1-octanol/water partition coefficients were calculated with the C log *P* program (version 4.0, BioByte, Clarement, USA) and data analysis was performed with the JMP program (version 6.0.0, SAS Inc., Cary, USA).

References and notes

1. Lipinski, C. A.; Lombardo, F.; Dominy, B. W.; Feeney, P. J. *Adv. Drug Deliv. Rev.* **1997**, *23*, 3.
2. van de Waterbeemd, H.; Smith, D. A.; Beaumont, K.; Walker, D. K. *J. Med. Chem.* **2001**, *44*, 1.
3. Bergström, C. A. S. *Expert Opin. Drug Metab. Toxicol.* **2005**, *1*, 613.
4. Delaney, J. S. *Drug Discovery Today* **2005**, *10*, 289.
5. Testa, B.; Avdeef, A. *Cell Mol. Life Sci.* **2002**, *59*, 1681.
6. Bevan, C. D.; Lloyd, R. S. *Anal. Chem.* **2000**, *72*, 1781.
7. Pan, L.; Ho, Q.; Tsutsui, K.; Takahashi, L. *J. Pharm. Sci.* **2001**, *90*, 521.
8. Chen, T. M.; Shen, H.; Zhu, C. *Comb. Chem. High Throughput Screening* **2002**, *5*, 575.
9. Avdeef, A. *Curr. Top. Med. Chem.* **2001**, *1*, 277.
10. Roy, D.; Ducher, F.; Laumain, A.; Legendre, J. Y. *Drug Dev. Ind. Pharm.* **2001**, *27*, 107.
11. Sugaya, Y.; Yoshiba, T.; Kajima, T.; Ishihama, Y. *Yakugaku Zasshi* **2002**, *122*, 237.
12. Erlanson, D. A.; McDowell, R. S.; O'Brien, T. *J. Med. Chem.* **2004**, *47*, 3463.
13. Leach, A. R.; Hann, M. M.; Burrows, J. N.; Griffen, E. J. *Mol. BioSyst.* **2006**, *2*, 429.
14. Albert, J. S.; Blomberg, N.; Breeze, A. L.; Brown, A. J. H.; Burrows, J. N.; Edwards, P. D.; Folmer, R. H. A.; Geschwindner, S.; Griffen, E. J.; Kenny, P. W.; Nowak, T.; Olsson, L.-L.; Sanganee, H.; Shapiro, A. B. *Curr. Top. Med. Chem.* **2007**, *7*, 1600.
15. Comess, K. M.; Schurdack, M. E. *Curr. Opin. Drug Discov. Devel.* **2004**, *7*, 411.

16. Hann, M. M.; Leach, A. R.; Harper, G. *J. Chem. Inf. Comput. Sci.* **2001**, *41*, 856.
17. SMARTS Manual, Daylight Chemical Information Systems Inc., 27401 Los Altos—Suite 360, Mission Viejo, CA 92691. http://www.daylight.com/dayhtml/doc/theory/theory.smarts.html.
18. Kogej, T.; Engqvist, O.; Blomberg, N.; Muresan, S. *J. Chem. Inf. Model.* **2006**, *46*, 1201.
19. Fini, A.; Fazio, G.; Hervás, M. F.; Holgado, M. A.; Rabasco, A. M. *Eur. J. Pharm. Sci.* **1996**, *4*, 231.
20. Pudipeddi, M.; Serajuddin, A. T. M. *J. Pharm. Sci.* **2005**, *94*, 929.
21. Kenny, P. W.; Sadowski, J. In *Chemoinformatics in Drug Discovery*; Oprea, T. I., Ed.; Wiley-VCH Verlag GmbH & Co.: Weinheim, 2005; pp 271–284.